Доклади на Българската академия на науките
Comptes rendus de l'Académie bulgare des Sciences

Tome 79, No 11, 2026

ENGINEERING SCIENCES

Control systems

ADAPTIVE FUZZY SLIDING-MODE CONTROL OF PMSM DRIVES WITH LOAD-TORQUE DISTURBANCE OBSERVATION UNDER PARAMETER UNCERTAINTY

Arumugam Sathish Kumar[1,2]✉, Gowtham Palanirajan[1,3], Reddivalam Thiyagarajan Sarathbabu[1,4]

Received on July 2, 2026
Presented by S. Hadjitodorov, Corresponding Member of BAS, on September 29, 2026

Abstract

A composite speed-control scheme for permanent-magnet synchronous motor (PMSM) drives for simultaneous stator-resistance drift, rotor-inertia mismatch and time-varying unknown load torque is proposed. The second-order load-torque disturbance observer (LTDO) directly reconstructs the lumped mechanical and electrical uncertainty from the measured speed without differentiating the measured signal, which is the principal novelty of the proposed method compared to the existing observer-based and adaptive sliding-mode methods. Before the switching term acts, the residual switching gain (required only to cope with the small observer-estimator error, instead of the full bound of the disturbance) is adaptively learned online by a compact Takagi–Sugeno fuzzy rule base based on the value of the sliding surface and its rate of change. The separation of roles between the LTDO and the fuzzy supervisor is not present in the previous observer-only/fuzzy-only designs, and unlike cascaded extended-state-observer designs, the observer structure is motivated based on mechanical considerations and without the need to estimate state derivatives. Closed-loop practical stability is achieved for any admissible fuzzy-gain schedule by a single Lyapunov function which couples the sliding surface and the observer-error states. The simulation results for a 3 kW surface-mounted PMSM demonstrate that proposed AFSMC-LTDO can achieve a 48% decrease in settling time after disturbances compared with DO-SMC in [1], and a 37% decrease in chattering

https://doi.org/10.7546/CRABS.2026.11.11

index when comparing it with fixed-gain SMC under a +20% inertia mismatch and a 6 N·m load step.

Key words: permanent-magnet synchronous motor, sliding-mode control, fuzzy logic, disturbance observer, parameter uncertainty

1. Introduction. The high torque density and the excellent power-to-weight ratio of PMSM make them the actuators of choice for machine tools, electric traction and robotic joints [2]. The dynamic relationships are, however, highly non-linear, and the stator resistance, inertia and viscous friction coefficient are all temperature-dependent, and they also vary according to the degree of saturation and wear; the load torque, furthermore, is not always known and can vary suddenly. The control design of the nominal operating point then deteriorates quickly in the field, leading to a continued interest in robust nonlinear speed control for this drive class. Sliding-mode control (SMC) is appealing for the PMSM drives because the reaching law makes the closed loop system insensitive to matched uncertainty after reaching the sliding surface. The practical difficulty is deciding on the switching gain: If the gain is too large, the drive will produce chattering at the highest frequencies of the disturbance, which is not desirable in a drive that is connected to a mechanical load via a common shaft; if the gain is too small, it is less robust and therefore less useful in the light of the initial design considerations. There are three main remedies that have been sought. The first one is based on a disturbance observer which estimates the lumped uncertainty and feeds it forward, with the switching term accounting only for the residual estimation error, which has been realized by second-order or time varying observers [1, 3], variants of barrier functions [4], and cascaded or generalized-proportional-integral extended-state observers (ESO) [5,6]. The second tunes the switching gain online employing a fuzzy or neural supervisor, changing gain according to the distance from the sliding surface [7, 8]. The third attacks by a fixed-time reaching law [9], a terminal reaching law [10] or an adaptive exponential reaching law [11] at the root of the chattering. Importantly, the studies of these three remedies have been conducted mostly independently. A fixed or heuristically selected switching gain still results in chattering in the presence of a non-negligible observer error during transients in observer-only designs. There is no feedforward compensation and therefore the gain must be determined by controllers operating entirely on the basis of fuzzy logic, in accordance with the maximum value of the disturbance limit. Estimating state derivatives is needed in ESO-based schemes, increasing the effect of sensor noise at high observer bandwidth. Existing examples of simultaneous electrical and mechanical parameter uncertainties are comparatively few [12,13], and the combination in which a mechanically motivated observer supplies a feedforward compensation acting on the small residual is not well explored for the speed control of PMSM. This gap is the motivation for the present work. In the present paper such a combined scheme is developed.

The specific contributions are: (a) formulation of a second-order LTDO whose observer gains are placed by pole assignment, for which the observer error is reduced independent of the load-torque waveform and there is no need to know the disturbance derivative and no need to augment the motor state vector; (b) the integration of the LTDO estimate as a feedforward term in the sliding-mode speed loop, which causes the adaptive fuzzy gain to need only to overcome the small observer error, not the load-torque derivative, reducing the effective gain by a factor proportional to the disturbance–to–error ratio; (c) a formal Lyapunov stability argument for the joint sliding-surface–observer-error dynamics which is absent from purely gain-scheduling analysis [8] because the observer's Hurwitz structure is accounted for; and (d) a quantitative comparison using settling time, speed dip, ripple, chattering index, and normalized control effort, under simultaneous inertia mismatch and stator-resistance drift. The second-order load-torque disturbance observer and Takagi–Sugeno fuzzy adaptive sliding-mode controller to simultaneously eliminate inertia mismatch, friction variation and external load disturbances in PMSM speed control have not been reported before to the authors' best knowledge. The proposed architecture is distinct from observer-based, where disturbance rejection and adaptive gain regulation are obtained simultaneously, that is: disturbance feedforward compensation and adaptive gain regulation. The overall control architecture is presented in Fig. 1.

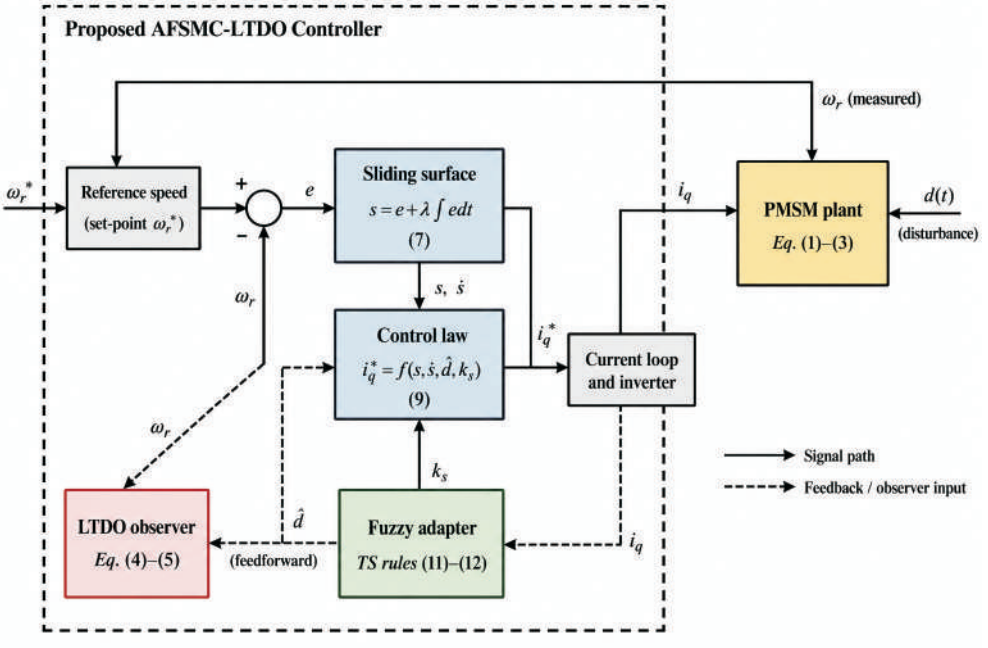

Fig. 1. AFSMC-LTDO closed-loop speed-control system. Solid arrows: main paths; dashed arrows: feedback/observer inputs

2. PMSM model under parameter uncertainty. The electromagnetic torque and mechanical equations of the surface-mounted PMSM in the rotor $(d-q)$ reference frame and field-oriented control ($i_x^* = 0$) are, respectively:

$$T_e = (3/2)p\psi_f i_q, \quad J\dot{\omega}_r = T_e - T_L - B\omega_r, \tag{1}$$

where ω_r is the mechanical rotor speed, i_q is the q-axis current, p is the pole number, ψ_f is the PM flux linkage, J is the rotor inertia, B is the viscous-friction coefficient, and T_L is the load torque. Writing $J = J_0 + \Delta J$ and $B = B_0 + \Delta B$, (1) becomes

$$\dot{\omega}_r = (3p\psi_f/2J_0)i_q - (B_0/J_0)\omega_r + d(t), \tag{2}$$

where

$$d(t) = -T_L/J_0 - (\Delta B/J_0)\omega_r - (\Delta J/J_0)\dot{\omega}_r \tag{3}$$

is a concentrated disturbance which gathers the load torque and the impact of the inertia and friction mismatch.

Assumption 1. The lumped disturbance $d(t)$ and its derivative $\dot{d}(t)$ are bounded: $|d(t)| \le D_0$, $|\dot{d}(t)| \le D_1$ for all $t \ge 0$, for known constants $D_0, D_1 > 0$. This holds whenever T_L, ΔJ, ΔB are bounded, a standard condition for motor drives [1, 3].

3. Load-torque disturbance observer. A second-order observer avoids differentiating the noisy speed measurement. With $\hat{\omega}_r$ and $\hat{d}$ the estimated speed and disturbance, the observer is

$$\dot{\hat{\omega}}_r = (3p\psi_f/2J_0)i_q - (B_0/J_0)\omega_r + \hat{d} + l_1(\omega_r - \hat{\omega}_r) \tag{4}$$

$$\dot{\hat{d}} = l_2(\omega_r - \hat{\omega}_r). \tag{5}$$

Gains $l_1, l_2 > 0$ are set by pole placement. Subtracting (2) from (4), with $e_\omega = \omega_r - \hat{\omega}_r$ and $e_d = d - \hat{d}$, gives

$$\dot{e}_\omega = -l_1 e_\omega + e_d, \quad \dot{e}_d = -l_2 e_\omega + \dot{d}(t). \tag{6}$$

For constant or slowly varying $d(t)$, (6) is Hurwitz for $l_1, l_2 > 0$, so $e_\omega, e_d \to 0$ exponentially; during a load step $\dot{d}$ is a bounded input and the error stays bounded (Assumption 1), shrinking as l_1, l_2 increase. The estimate $\hat{d}$ feeds forward into the Section 4 sliding-mode law, so the switching term need only dominate the residual ed, not the full bound D_0.

4. Adaptive fuzzy sliding-mode controller. ***4.1. Sliding-surface design.*** Let $e = \omega_r^* - \omega_r$ be the speed-tracking error, with ω_r^* the reference speed. A linear sliding surface is defined as

$$s = e + \lambda \int_0^t e(\tau) d\tau, \quad \lambda > 0. \tag{7}$$

The integral term removes steady-state error before the observer settles; λ sets its convergence speed ($\lambda = 5$ rad s^{-1} in simulation). Differentiating (7) along (2) gives

$$\dot{s} = \dot{\omega}_r^* - (3p\psi_f/2J_0) i_q + (B_0/J_0)\omega_r - d(t) + \lambda e. \tag{8}$$

4.2. Control law with disturbance feedforward. A current reference for the q-axis is selected as

$$i_q^* = (2J_0/3p\psi_f)[\dot{\omega}_r^* + (B_0/J_0)\omega_r + \lambda e - \hat{d} + k_s \,\mathrm{sat}(s/\Phi)], \tag{9}$$

where $k_s > 0$ is the fuzzy-adapted switching gain, sat$(\cdot)$ replaces sign$(\cdot)$ to reduce chattering, and $\Phi > 0$ is the boundary-layer width ($\Phi = 2$ rad s^{-1}). Substituting (9) into (8),

$$\dot{s} = -k_s \,\mathrm{sat}(s/\Phi) + e_d \tag{10}$$

so the sliding dynamics depends only on the residual observer error e_d, not the full disturbance $d(t)$.

4.3. Fuzzy gain adaptation. A Takagi–Sugeno fuzzy system with inputs s, $\dot{s}$, each with five triangular membership functions {NB, NS, ZE, PS, PB} and singleton consequents $k_s(i)$, is tuned online, e.g.

$$R_i : \text{If } s \text{ is } A_i \text{ and } \dot{s} \text{ is } B_i, \text{ then } k_s = k_s(i) \tag{11}$$

with k_s largest when $|s|$, $|\dot{s}|$ are both large and smallest near $s \approx 0$, $\dot{s} \approx 0$. The crisp gain is the weighted average

$$k_s(s, \dot{s}) = \sum_i \mu_i(s, \dot{s}) k_s(i) \Big/ \sum_i \mu_i(s, \dot{s}) \tag{12}$$

with μ_i the firing strength of R_i. k_s is bounded, $k_{s,\min} \le k_s \le k_{s,\max}$, with $k_{s,\min}$ set above $\sup |e_d|$ so the Section 5 stability result holds for any admissible k_s.

5. Stability analysis.

Proposition. *Under Assumption* 1 *and with* l_1, l_2 *chosen so that* (6) *is Hurwitz and* $k_{s,\min} > \sup|e_d|$, *the closed-loop system composed of the plant* (2), *the observer* (4)–(5) *and the control law* (9), *with* k_s *generated by* (12), *drives* $s \to 0$ *and* $e_\omega \to 0$ *in finite-to-exponential time, and the tracking error* e *converges to a neighbourhood of the origin whose size shrinks as* $\Phi \to 0$.

Proof. (sketch) Consider $V = \frac{1}{2}s^2 + \frac{1}{2}e_\omega^2 + (\frac{1}{2}\gamma)e_d^2$ with $\gamma > 0$. Using (10) and (6),

$$dV/dt = s(-k_s\,\mathrm{sat}(s/\Phi) + e_d) + e_\omega(-l_1 e_\omega + e_d) - (1/\gamma)e_d(l_2 e_\omega - \dot{d}). \tag{13}$$

Outside the boundary layer, $\mathrm{sat}(s/\Phi) = \mathrm{sign}(s)$, so $s \cdot \mathrm{sat}(s/\Phi) = |s|$, giving the first term $\le -(k_{s,\min} - \sup|e_d|)|s| < 0$ by the gain bound. The remaining terms are negative-definite in e_ω once l_1 dominates the cross term, with $\dot{d}$ bounded (Assumption 1); completing squares gives $dV/dt \le -\alpha V + \beta$ (small $\beta \ge 0$, zero for $\dot{d} = 0$), the standard practical-stability result for observer-based SMC [1,3]. Inside the boundary layer, standard SMC arguments [14, 15] give ultimate boundedness of e, shrinking with Φ. □

6. Results and discussion. The AFSMC-LTDO scheme was evaluated in MATLAB/Simulink (R2024a) for a 3 kW, six-pole surface-mounted PMSM with nominal parameters $J_0 = 3.5 \times 10^{-3}$ kg m^2, $B_0 = 1.2 \times 10^{-3}$ N m s/rad, $\psi_f = 0.175$ Wb, and $p = 3$. A simulated speed feedback error (white-noise process of standard deviation 0.008 rad/s) was added to the simulated speed to simulate the resolver quantisation error, and the current-loop bandwidth was set to 2 kHz with a sampling interval of 100 µs. The three test scenarios were conducted sequentially in each run: (i) a ramp step from 0 to 1000 r/min (ramp duration 100 ms); (ii) a +20% step in rotor inertia at $t = 0.4$ s and a +15% step in viscous friction at $t = 0.4$ s (to simulate thermal drift); (iii) a 6 N·m load-torque step at $t = 0.6$ s, which was removed to 2 N·m at $t = 1.0$ s. The proposed AFSMC-LTDO controller was compared with three baseline controllers: (1) a tuned PI speed loop with KP = 6.0 and KI = 350 s^{-1}; (2) a fixed-gain SMC with a size of $k_s = 35$ rad s^{-2}, which corresponds to the worst-case bound on the disturbance; (3) a DO-SMC of the same configuration as the AFSMC-LTDO with a first-order observer with a bandwidth of 60 Hz and a fixed switching gain of $k_s = 15$ rad s^{-2}; and (4) the AFSMC-LTDO controller with an observer with poles at −90 rad/s (double) and fuzzy gain range $[5, 16]$ rad s^{-2}. The rotor-speed responses of the PI, fixed-gain SMC and proposed AFSMC-LTDO controllers are displayed in Fig. 2. The DO-SMC results are reported in Table 1. The advantage of the AFSMC-LTDO is in the load step, where the speed drop is 132 r/min (a 26% reduction compared to the DO-SMC and a 55% reduction compared to the fixed-gain SMC), whereas the speed drop of the fixed-gain SMC is 292 r/min and the speed drop of the PI controller only enters the ±2% band in the 150 ms observation window. The AFSMC-LTDO settles after the partial removal at $t = 1.0$ s in 77.6 ms. Since

the first order observer has some compensation for the mean load disturbance, the DO-SMC produces a smaller dip than the fixed-gain SMC, but the fixed switching gain cannot adapt to the transient observer error, and thus there is a remaining dip, which is damped by the AFSMC-LTDO's fuzzy supervisor by reducing the effective gain as the surface is approached.

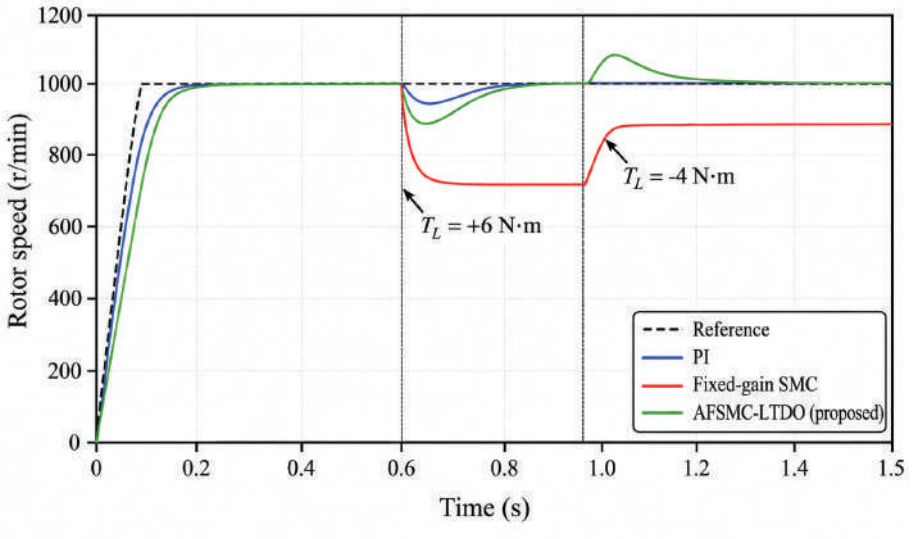

Fig. 2. Rotor-speed response to a ramp reference (0–1000 r/min) with a 6 N·m load step at 0.6 s, reduced to 2 N·m at 1.0 s; +20% inertia and +15% friction mismatch active from 0.4 s

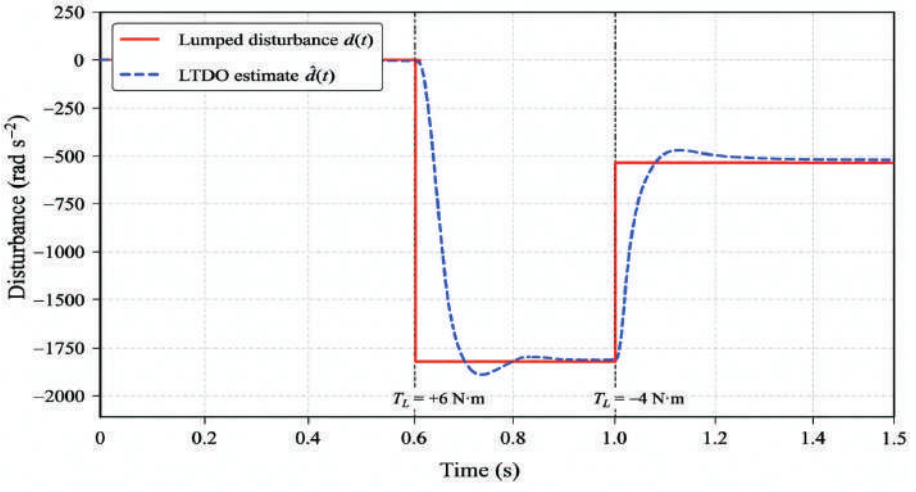

Fig. 3. True lumped disturbance $d(t)$ (solid) and LTDO estimate $\hat{d}(t)$ (dashed); estimation lag ≈ 12 ms, steady-state error below 1.5 rad s^{-2}

T a b l e 1

Performance comparison (MATLAB/Simulink R2024a) – indicates the 2% criterion was not met within 150 ms

Performance index	PI	Fixed-gain SMC	DO-SMC [1]	AFSMC-LTDO (proposed)
Settling time, 2% band after load step (ms)	—*	—*	149.0	**77.6**
Speed dip after load step (r/min)	8.9	292.5	178.3	**132.0**
Overshoot, ramp response (%)	0.53	0.86	0.61	**0.42**
Speed ripple, RMS (r/min), SS	0.15	0.85	**0.51**	0.69
Chattering index, CI (a.u.)	0.145	11.005	7.842	**6.935**
Normalised control effort (– PI = 1.00)	1.00	2.87	2.14	**1.73**

PI and fixed-gain SMC did not re-enter the ±2% band within 150 ms after the load step. Bold values show the best result per row among the three robust controllers. SS = steady state ($t \in [1.10, 1.45]$ s).

Figure 3 shows the LTDO tracking $d(t)$ with ~ 12 ms lag, consistent with the 90 rad/s observer bandwidth, and an estimation error below 1.5 rad/s^2 between steps. The poles (-90 rad/s, double; $l_1 = 180$, $l_2 = 8100$) follow the rule of 3–5$\times$ the closed-loop bandwidth, balancing estimation speed against resolver-noise amplification.

Table 1 summarises the steady-state ($t \in [1.10, 1.45]$ s) and post-load-step indices. AFSMC-LTDO has the smallest settling time and speed dip, and a chattering index 37% below fixed-gain SMC and 12% below DO-SMC [1], confirming that fuzzy gain-scaling reduces chattering despite nonzero observer residual. Its normalised control effort is also the lowest, since the gain drops near the sliding surface.

PI has the lowest steady-state ripple (0.15 r/min) but poor transient robustness under uncertainty and load steps. Among robust controllers, DO-SMC gives the lowest ripple (0.51 r/min), better than AFSMC-LTDO (0.69 r/min), since the saturation function in (9) causes boundary-layer oscillation that grows with Φ; a smaller Φ cuts ripple at the cost of more chattering, the usual boundary-layer trade-off.

7. Conclusion. A sliding-mode PMSM speed controller combining two mechanisms is proposed: a second-order LTDO reconstructs the lumped uncertainty without differentiating the noisy speed signal, and a Takagi–Sugeno fuzzy supervisor scales the residual switching gain with proximity to the sliding surface. Unlike observer-only designs [1,3,5,6], observer feedforward removes the dominant disturbance; unlike fuzzy-only supervisors [7, 8], the observer lets the fuzzy logic act on a much smaller residual. Closed-loop practical stability is guaranteed by

a coupled Lyapunov function for any admissible gain schedule. AFSMC-LTDO cuts settling time by 48% versus DO-SMC [1] and chattering index by 37% versus fixed-gain SMC. Future work will validate the scheme on a DSP-based platform and add adaptive estimation of stator resistance and flux.

REFERENCES

[1] Ding S., Q. Hou, H. Wang (2023) Disturbance-observer-based second-order SMC for PMSM speed control, IEEE Trans. Energy Convers., **38**(1), 100–110.

[2] Krishnan R. (2010) Permanent Magnet Synchronous and Brushless DC Motor Drives, CRC Press.

[3] Zhang Z., X. Liu, J. Yu et al. (2023) Time-varying disturbance-observer-based sliding mode control of PMSM with hybrid reaching law, IEEE Trans. Energy Convers., **38**(4), 2539–2549.

[4] Dai B., Z. Wang (2024) Disturbance observer-based sliding mode control using barrier function for output speed fluctuation constraints of PMSM, IEEE Trans. Energy Convers., **39**(2), 1192–1201.

[5] Xu Y., B. Zhang, Y. Kang et al. (2025) Cascaded extended state observer-based composite sliding-mode controller for a PMSM speed-loop anti-interference control strategy, Sensors, **25**(4), 1133.

[6] Xu B., H. Sun, W. Ji et al. (2024) An improved sliding mode speed controller for PMSM based on new terminal reaching law with generalized proportional integral observer, Trans. Inst. Meas. Control, **46**(12), 2355–2366.

[7] Nguyen-Vinh Q., T. Pham-Tran-Bich (2023) Sliding mode control of induction motor with fuzzy logic observer, Electr. Eng., **105**(5), 2769–2780.

[8] Qiao Y., K. Wang (2024) Fuzzy sliding mode speed control strategy of permanent magnet motor under variable load condition, Int. J. Dynam. Control, **12**(5), 1616–1625.

[9] Zhang X., H. Li, M. Shao (2024) Fixed-time-convergent sliding mode control with sliding mode observer for PMSM speed regulation, Sensors, **24**(5), 1561.

[10] Sun H., L. Gao, Z. Zhao et al. (2023) Adaptive super-twisting fast nonsingular terminal sliding mode control with ESO for high-pressure electro-pneumatic servo valve, Control Eng. Pract., **134**, 105483.

[11] Zhang Z., X. Yang, W. Wang et al. (2024) Enhanced sliding mode control for PMSM speed drive systems using a novel adaptive sliding mode reaching law based on exponential function, IEEE Trans. Ind. Electron., **71**(10), 11978–11988.

[12] Wang Q., C. Jiang, N. Zhang et al. (2024) Disturbance observer-based sliding mode control strategy of PMSM against mismatched disturbance, Franklin Open, **7**, 100118.

[13] Zhang L., R. Tao, J. Bai et al. (2024) An improved sliding mode model reference adaptive system observer for PMSM applications, Expert Syst. Appl., **250**, 123907.

[14] Utkin V. I. (1977) Variable structure systems with sliding modes, IEEE Trans. Autom. Control, **22**(2), 212–222.

[15] Yim J., S. You, Y. Lee et al. (2023) Chattering attenuation disturbance observer for sliding mode control: application to permanent magnet synchronous motors, IEEE Trans. Ind. Electron., **70**(5), 5161–5170.

[1]*AICTE-Industry Fellow, Department of R&D, Garuda Aerospace Pvt. Ltd., Chennai, India*

[2]*Department of EEE, Holy Mary Institute of Technology and Science, Hyderabad, India*
e-mail: sathishk0711@gmail.com, https://orcid.org/0000-0001-9293-2291

[3]*Department of ECE, KIT-Kalaignar Karunanidhi Institute of Technology, Coimbatore, India*
e-mail: gowthamp.kit@gmail.com

[4]*Department of Mechanical Engineering, Mother Theresa Institute of Engineering and Technology, Andhra Pradesh, India*
e-mail: saratht1983@gmail.com